Laser Cladding of Iron-Base Alloy on Al-Si Alloy and Its Relation to Cracking at the Interface

A. Wang, C. Fan, C. Xie, W. Huang, and K. Cui

The present study established the basic operating range and diagram for cladding, by means of a laser, a cast Al-Si alloy substrate with an iron-base material. Considering that the main difficulty was interface cracking during this processing, the factors affecting the interface cracking ratio (ICR) were investigated from two aspects: the laser processing parameters (e.g., laser power, traverse speed, powder-feed rate, preheating temperature of the substrate, tempering temperature) and the material factor, including the composition of clad. The substrate temperature and the tempering temperature were found to be important for controlling ICR, and the content of Al and Ni in the clads also had significant influence on ICR. The intermetallic compounds formed in the interface region were analyzed to understand the effect of Ni content on ICR. Clads of thickness from 1.2 to 1.5 mm that were crack free and had good fusion were achieved by controlling the substrate temperature or adjusting the Al content in the clads.

Keywords
aluminum-silicon alloys, cladding, interface cracking, laser

1. Introduction

ALUMINUM alloys are being used to an increasing extent, especially as cast components for automotive or aircraft applications, owing to their light weight, high thermal conductivity, good corrosion resistance, and moderate mechanical properties. Unfortunately, the surface properties of aluminum alloy suffer because of low hardness, high coefficient of friction, and poor wear resistance (Ref 1). So far, there is a great interest in improving the wear resistance of aluminum alloys be means of surface modification. Among the various surface modification treatments, laser surface treatment is a new candidate technique.

Four kinds of techniques have been developed for laser treatment of aluminum alloys: laser shock hardening, laser remelting, laser alloying, and laser cladding. Laser shock hardening and laser remelting treatments can produce only moderate increases in surface strength and hardness. Laser alloying treatment can generate a hard alloyed layer (with a Vickers hardness of 600 to 800 HV), but some drawbacks, such as porosity, cracks, and inclusions, are difficult to eliminate in the alloyed layer, since the intense reactions between melted aluminum and the atmosphere or additional elements may cause either oxidization or formation of intermetallic compounds during the laser alloy process (Ref 2). In the laser cladding process, the substrate is just melted and covered by the melted powder rapidly, so the intense reactions occurring during the laser alloying process can be reduced to some extent. Therefore, most investigations have been concentrated on laser cladding of aluminum alloys in recent years (Ref 3-5).

Up to now, Ni-, Co-, and Cu-base alloys have been evaluated as materials for the cladding of aluminum alloys (Ref 3-6). It is well known that aluminum can form many intermetallic phases with elements such as Ni, Co, Cr, Fe, and Cu, thus producing an interface region where one or more brittle intermetallic compounds may be expected. This interface region is susceptible to cracking due to the brittleness of intermetallics (Ref 5, 6), so control of brittleness at the interface becomes an important aspect of the quality of clads. In the present work, laser cladding of Fe-base alloy (a less commonly used clad material) on an Al-Si alloy and its relation to cracking at the interface were investigated.

A. Wang, C. Fan, C. Xie, W. Huang, and **K. Cui,** Department of Materials Science and Engineering, Huazhong University of Science and Technology, Wuhan, 430074, P.R. China.

2. Experimental Procedure

Compositions for the cladding and substrate materials are listed in Table 1. The clads were produced by means of a homemade powder autofeeding apparatus and a 2 kW CW CO_2 laser. The laser beam was defocused by a GaAs lens onto the samples to be laser clad, while N_2 gas flowed axially to the laser beam axis to protect the lens from the melted and vaporized materials. Liu (Ref 4) has used the sandpaper polishing method and the sandblasting method to remove Al_2O_3 film from the substrate surface. Results showed that the sandpaper-polished surface possessed a smaller dilution than the sandblasted surface because the sandpaper-polished surface had a lower absorption to the laser beam in front of the laser-generated powder pool than that of the sandblasted substrate. Therefore, the aluminum alloy samples, $35 \times 70 \times 10$ mm^3, were cleaned with sandpaper in our experiment.

The as-clad specimens were cross sectioned for optical microscopy and SEM EDX analysis. The clad coatings were exfoliated parallel to the substrate surface to retain different thickness of coatings for X-ray diffraction analysis.

3. Results

3.1 *Basic Operating Range and Diagram for Laser Cladding of WF312 Alloy on ZL108 Alloy*

The material factors and the processing parameters are two kinds of important aspects affecting the quality of clads (Ref 4). When the materials for coating and substrate are determined,

Table 1 Compositions of the clads and the substrate

Name of materials (a)	Element, wt%										
	C	B	Mg	Al	Si	Cr	Mn	Fe	Ni	Cu	Mo
WF312 (clad)	0.2	1.5	...	...	4.3	21.1	...	bal	12.5	1.4	1.4
Ni35 (clad)	0.7	2.1	...	...	4.1	16.9	...	5.4	bal	...	...
ZL108 (substrate)	...	...	2.1	bal	13.2	...	0.52	...	1.3	1.3	...

(a) Commercial names of materials used in China

Table 2 Laser parameters used in this experiment

Parameter	Values
P, kW	1.6, 1.8, 2.0
d, mm	4, 5, 6
V_s, mm/s	2, 4, 6, 8
G, mg/mm	20, 30, 40, 60

the clad formation is influenced chiefly by laser processing parameters: P (laser power), d (laser spot size), V_p (powder-feed rate), V_s (traverse speed), and V_g (flow rate of assisting gas). The parameters used in this experiment are listed in Table 2.

If P and G were kept at 2 kW and 20 mg/mm, respectively, and laser spot size was 5 or 6 mm in diameter, the traverse speeds lower than 2 mm/s produced continuous clads, but long interaction time between the laser beam and the substrate (about 2.5 to 3.0 s) resulted in a large portion of laser energy penetrating into the substrate and induced overmelting of the substrate. Cracks observed by visual examination in the produced coatings (because of the brittleness of intermetallic compounds and a high value of microhardness, up to 800 to 850 HV compared with the microhardness of the WF312 materials, about 450 HV, due to the hardening effect of hard intermetallic compounds) indicated that the process was laser alloying rather than laser cladding. On the other hand, traverse speeds larger than 2 mm/s generated discontinuous clads. Furthermore, when the laser spot size was reduced to 4 mm in diameter and G was 20 mg/mm, laser power changing from 1.6 to 2.0 kW and traverse speeds between 4 and 8 mm/s produced good clad tracks. It can be deduced that the basic conditions to form good clads are as follows:

$$Q_0 \geq 127 \text{ W/mm}^2 \quad \text{(Eq 1)}$$

$$\tau \leq 1 \text{ s} \quad \text{(Eq 2)}$$

where $Q_0 = 4P/(\pi d^2)$, laser power density; and $\tau = d/V_s$, the interaction time between laser beam and substrate.

Under the above conditions, the laser spot size was kept at 4 mm in diameter while other parameters were arranged according to Table 2 in our later experiments. Figure 1 shows the basic operating diagram for laser cladding of WF312 alloy on ZL108 alloy. It can be found that E and G had great influence on the macroquality of clads and that good clads could be produced under the following condition:

$$E \geq 47.6 + 1.3G \quad \text{(Eq 3)}$$

where $E = P/(dV_s)$ (J/mm^2). Therefore, Eq 1 to 3 represent the operating range of laser processing parameters under the present experimental condition. The thickness of clads were 1.2, 1.5, and 1.8, corresponding to G = 20, 30, and 40 mg/mm, respectively.

3.2 *Factors Affecting the ICR*

Good clads produced under the above operating ranges were cross sectioned for microscopy. Three regions in a typical clad track were observed: the clad region, the interface region, and the postmolten region, as shown in Fig. 2. The interface region is a solidified region composed of the mixture of clad material and melted substrate. The postmolten region is a special zone generated in this cladding system. The ZL108 alloy has a lower melting point, about 580 °C, compared with the melting points of the clad region (about 1150 °C) and the interface region (the melting point depends on its composition). As the molten pool (clad region and interface region) solidified, it released latent heat that penetrated into the substrate and heated up the substrate to cause a molten layer of substrate adjacent to the interface region. Thus the name "postmolten region." SEM EDX analysis of the postmolten region (as shown in Table 3) compared with the composition of the substrate (see Table 1) confirmed that the composition of the postmolten region was unaffected by the clad material.

In the interface region, aluminum may interact with Fe, Ni, and Cr elements existing in the clad material and form some brittle intermetallic phases. Therefore, some cracks were also found in the interface region, which has the same characteristics as the laser-clad Ni-, Co-, and Cu-base alloy coatings on aluminum alloys studied by previous investigators (Ref 3-6), as shown in Fig. 3(a).

Here we introduce the concept of an interface cracking ratio (ICR) to evaluate the cracking extent in the interface region. It can be expressed as follows:

$$\text{ICR} = \frac{\sum_{i=1}^{N} L_i}{W} \times 100\% \quad \text{(Eq 4)}$$

where W is the width of clads and L_i is the length of each separate crack projecting on the originally unmolten surface of substrate, as shown in Fig. 3(b).

When d and G were kept at 4 mm and 20 mg/mm, respectively, an L_9 (3^4) orthogonal array was adopted to investigate four major factors affecting ICR: P, V_s, T_p (preheating tempera-

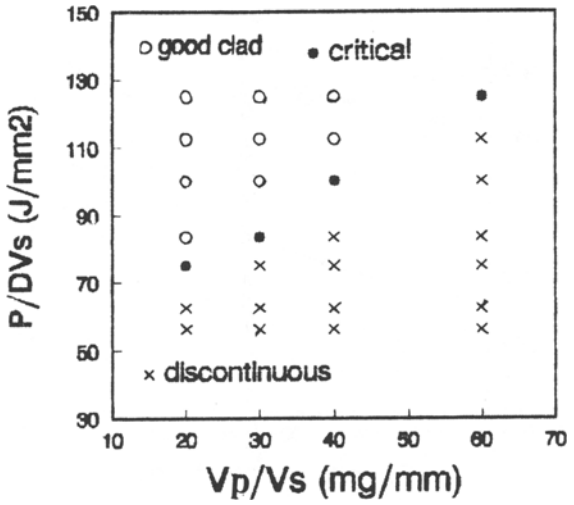

Fig. 1 The operating diagram for laser cladding of iron-base alloy on Al-Si alloy

Table 3 SEM EDX composition analysis of the postmolten region

Element	wt%
Mg	1.8
Al	bal
Si	12.8
Mn	0.40
Ni	1.23
Cu	1.7

Table 4 The orthogonal array for ICR investigation

Trial No.	P, kW	V_s, mm/s	T_p, °C	T_t, °C	ICR, %
1	1.6(1)	4(1)	0(1)	0(1)	39.6
2	1.6(1)	6(2)	200(2)	200(2)	76.5
3	1.6(1)	8(3)	400(3)	400(3)	0
4	1.8(2)	4(1)	200(2)	400(3)	11.8
5	1.8(2)	6(2)	400(3)	0(1)	3.8
6	1.8(2)	8(3)	0(1)	200(2)	100.0
7	2.0(3)	4(1)	400(3)	200(2)	9.1
8	2.0(3)	6(2)	0(1)	400(3)	15.9
9	2.0(3)	8(3)	200(2)	0(1)	25.8
I/3	38.7	20.2	51.8	23.1	...
II/3	38.5	32.1	38 0	61.9	...
III/3	16.9	41.9	4.3	9.2	...
Range	21.8	21.7	47.5	52.7	...

ture of substrate) and T_t (tempering temperature) as shown in Table 4.

It can be seen from Table 4 that T_p and T_t had more significant effects on ICR than P and V_s, and that the interfacial crack-free coating could be produced under the following optimized parameters: P = 2 kW, V_s = 4 mm/s, and $T_p = T_t$ = 400 °C.

3.3 *Effect of the Substrate Temperature on ICR*

During the laser cladding process, the temperature of the substrate (T_s) just beneath the laser irradiated zone increases. In order to investigate the effect of T_s on clad quality, four Pt-Rh thermocouples were welded on the samples at locations A, B, C, and D as shown in Fig. 4, and then four X-Y recorders were connected to four thermocouples separately. The center of clad track was just 5 mm away from the side face of the substrate on

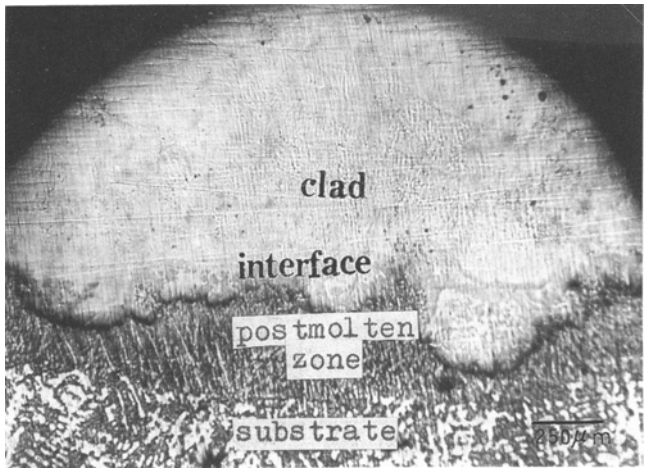

Fig. 2 Cross section of laser-clad coating

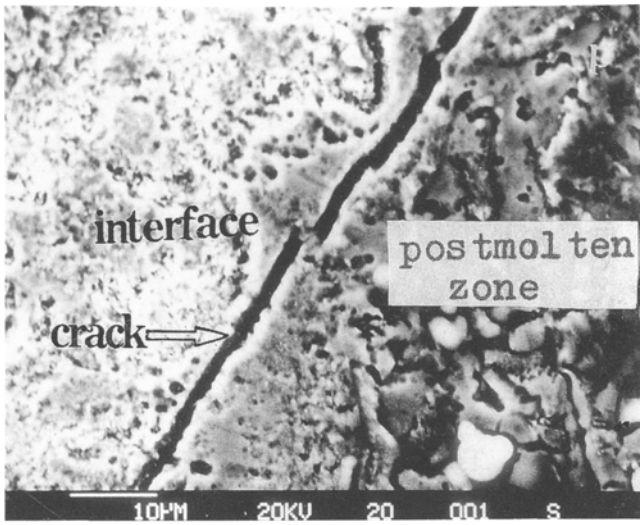

(a)

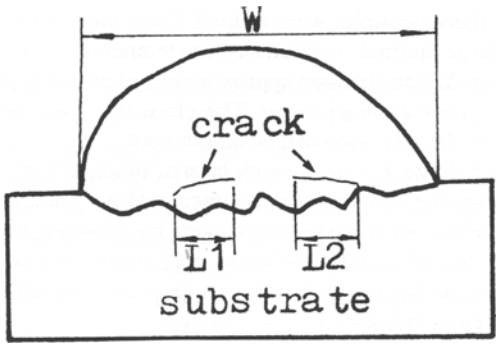

(b)

Fig. 3 Crack at the interface. (a) Morphology of crack at the interface. (b) Schematic illustration for the calculation of ICR

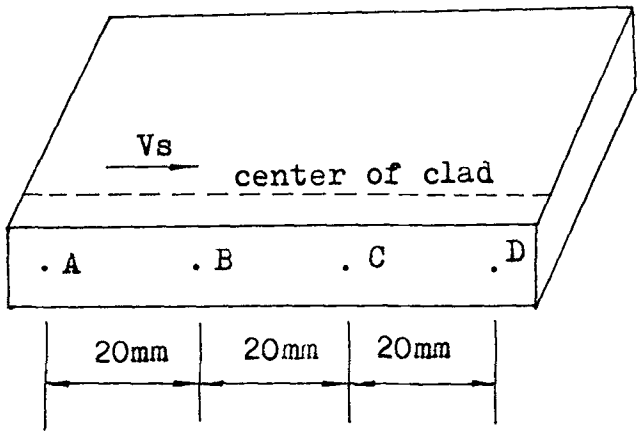

Fig. 4 Schematic illustration for measuring the temperature of substrate

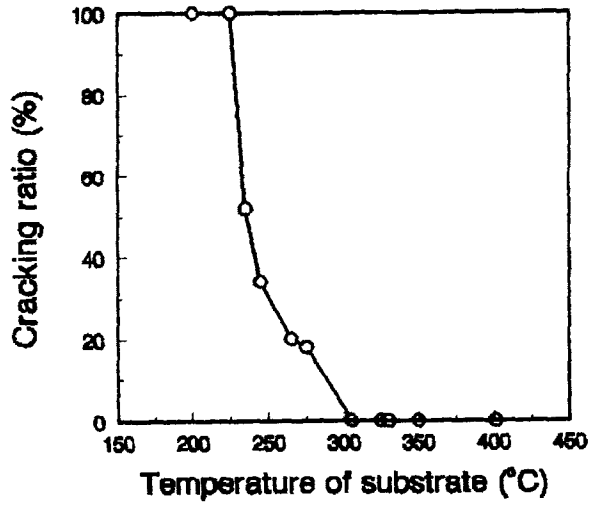

Fig. 6 ICR as a function of T_S

which the thermocouples were welded. Since the aluminum alloy has a large thermal conductivity, the temperature values recorded by X-Y recorders can approximately express the change in T_s during the cladding process. Therefore, the T_s just beneath the laser-irradiated region can be determined.

Figure 5 shows T_s varying with laser scanning length at different preheating temperatures. It indicates that T_s increased by 100 °C when the laser beam passed along the substrate from the beginning to end at three different preheating temperatures, and that the higher the preheating temperature, the higher the substrate temperature.

The cross sections of clads at different laser scanning lengths were observed with an optical microscope to measure the crack length at the interface. Results show that ICR reduced rapidly with increasing laser scanning length and increasing preheating temperature, and that interface cracking was eliminated when T_s was up to about 310 °C, as shown in Fig. 6. However, T_s larger than 380 °C could induce cracking in the clad region, because the overmelting of substrate caused large dilution and some brittle intermetallic compounds formed in the clad region.

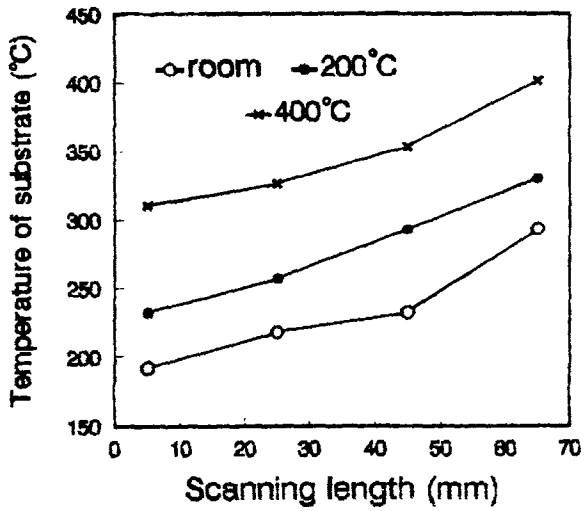

Fig. 5 The temperature of substrate changing with scanning length and preheating temperature

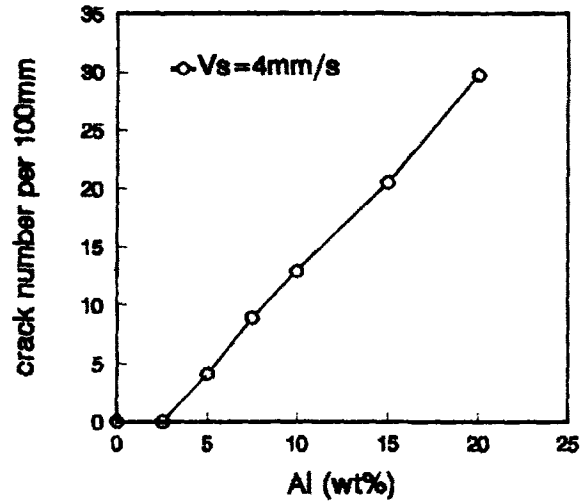

Fig. 7 The number of traverse cracks per 100 mm affected by Al content in the clads (preplaced powder)

3.4 *Effect of Al and Ni Content on ICR*

WF312 alloys mixed with different contents of pure Al powder (WF312 + 2.5 wt% Al, 5 wt% Al, 7.5 wt% Al, 10 wt% Al, and 15 wt% Al) were preplaced on ZL108 alloy substrate with a binder for laser cladding treatment to investigate the effect of Al content on ICR. A macrocheck of clads showed that cracks perpendicular to the direction of traverse speed (called traverse cracks) could be observed in these coatings containing Al. Figures 7 and 8 indicate that the crack number per 100 mm clad length increased with increasing Al content, and Al content also had a great influence on ICR (i.e., ICR reduced sharply with increasing Al content from 0 to 5 wt% and changed slightly with increasing Al content from 5 to 10 wt%).

Based on the above experimental results, further investigation was concentrated on the WF312 coatings containing Al from 0 to 3 wt% by the powder autofeeding method. Figure 9 shows that clads with Al content below 1 wt% could limit trav-

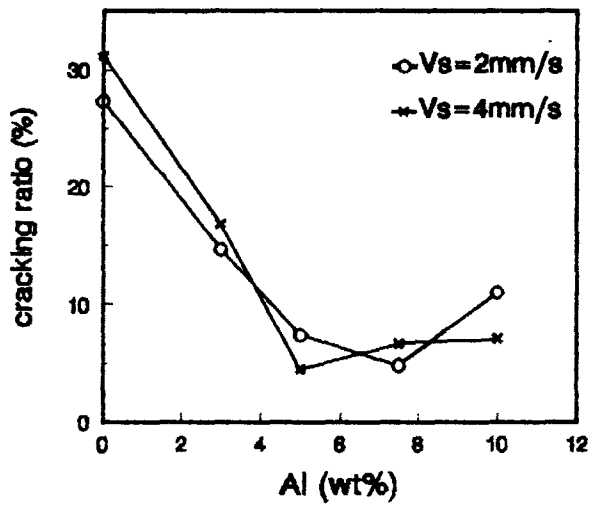

Fig. 8 ICR as a function of Al content

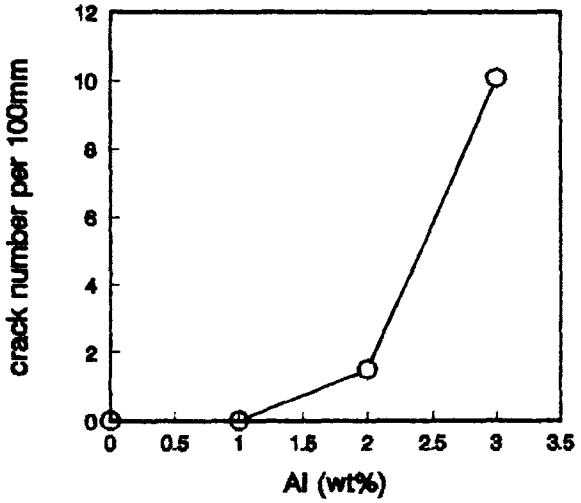

Fig. 9 The number of traverse cracks in the clads per 100 mm affected by Al content in the clads (autofeeding powder)

Table 5 Compositions of coatings with different Ni contents, wt %

Base alloy	WF312				Ni35
Added Ni content	0.0	10.0	20.0	30.0	0.0
Ni content	12.5	21.2	30.0	38.7	70.8
Fe content	57.6	51.8	46.1	40.3	5.4

erse cracking in the clad region while increasing Al content from 2 to 3 wt% induced significant traverse cracking. It is interesting to note that the interfacial cracking was eliminated completely in the clads containing 1 to 3 wt% Al, produced by the powder autofeeding method.

Ni was also added to the WF312 coatings to study its effect on ICR. The compositions designed are shown in Table 5. The powder autofeeding method was used. Results show that spallation of clads from the substrate along the interface zone, which means that ICR is 100%, was a major drawback in these coatings. The spallation of clads occurred at the beginning stage of the cladding process, and the spalling length of clads increased with increasing Ni content in the alloy coating, as shown in Fig. 10. Therefore, an increase of Ni content in the clads would increase the cracking susceptibility at the interface.

3.5 *X-ray Diffraction and SEM Analysis*

The clads were exfoliated from the substrate parallel to the substrate surface to retain three different thickness of clads: 0.5, 0.2, and 0.0 mm. The thickness of clads was defined as the distance from the surfaces of retained coating to the original substrate surface. The place where the thickness of the clad is 0 mm actually belongs to the interface region. X-ray diffraction of the exfoliated surfaces (see Fig. 11) shows that Al_3Ni and Al phase began to appear when the clads were thinned to about 0.2 mm and that the amount of Al_3Ni and Al phase increased and a new phase AlNi formed with thinning of the clads from 0.2 to 0 mm. The microhardness profile along the depth of clads shows that the interface region displayed a high peak value (about 600

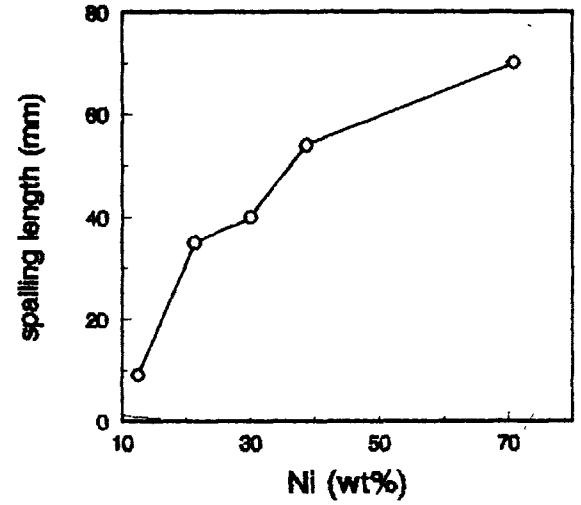

Fig. 10 Spalling length of clads changing with Ni content

to 800 HV) contributed by the hardening of intermetallic compounds, as shown in Fig. 12.

The composition-profile trace obtained by SEM EDX analysis at the central line of clads perpendicular to the substrate surface (see Fig. 13) shows that: the clad region showed a very uniform composition distribution and was undiluted by the substrate; the composition of postmolten region was the same as that of the substrate; the composition changed gradually from the postmolten region to the clad region; and the diffusive width changed only a little (from 0.2 to 0.25 mm) with increasing T_s from 200 to 300 °C.

4. Discussion

During the cladding process, a large thermal stress in the interface region was produced for the large difference of thermal expansion between the clad and the substrate (about 13×10^{-6} and 25×10^{-6} m/mK, respectively) and the high cooling rate

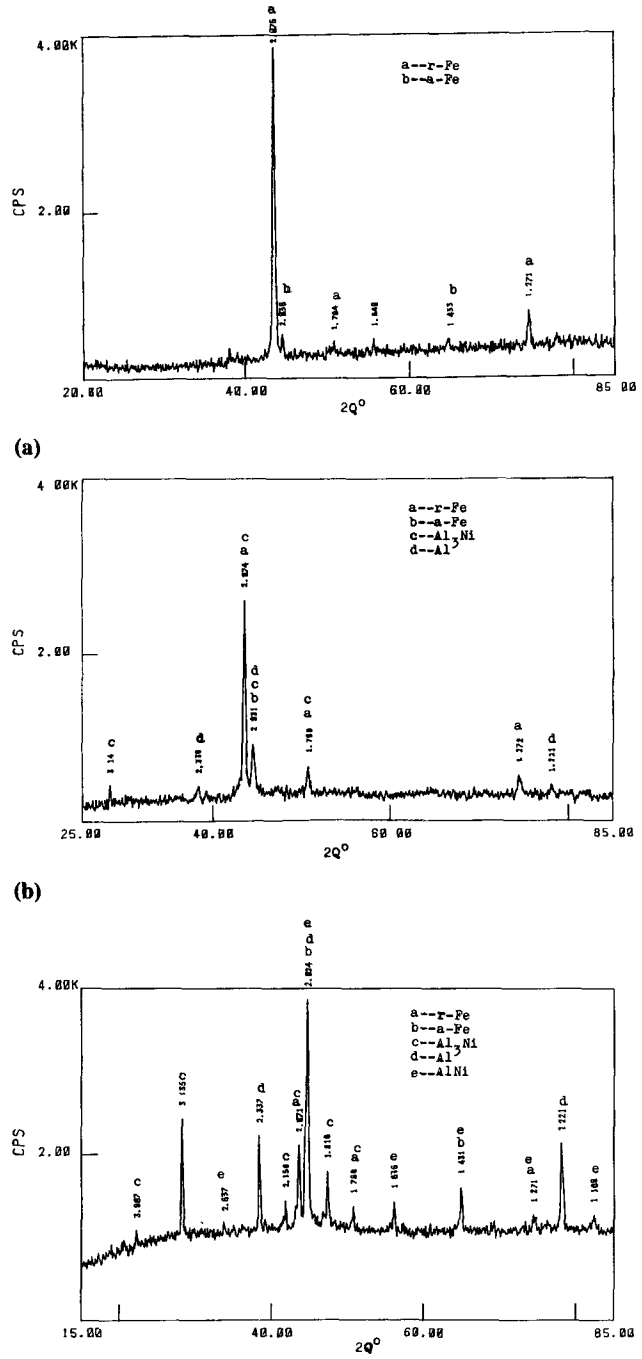

Fig. 11 X-ray diffraction spectrums of laser-clad Fe-base coating with different thicknesses. (a) 0.5 mm. (b) 0.2 mm. (c) 0.0 mm

(about 10^5 K/s) caused by the high thermal conductivity of aluminum alloy and the short interaction time between laser beam and substrate. For a cold substrate and no stress relaxation, such stress σ can be estimated by the following expression (Ref 7):

$$\sigma = \frac{E_c E_s \delta_c \Delta T}{E_c + E_s} \quad \text{(Eq 5)}$$

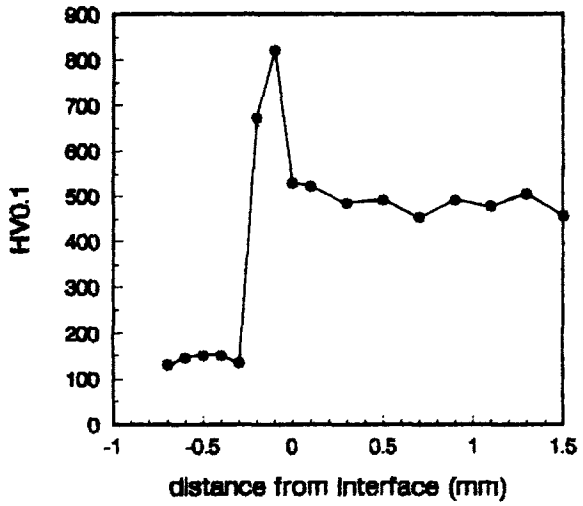

Fig. 12 Microhardness profile along the depth of clads

where E is the elastic modulus, δ is the thermal expansion coefficient, ΔT is temperature change after solidification, and subscripts c and s refer to clad and substrate, respectively. When $E_s = E_c = 2 \times 10^5$ MPa, $\Delta T = 800$ °C, and $\delta_c = 13 \times 10^{-6}$ m/mK, the thermal stress would reach $\sigma = 1040$ MPa. The high thermal stress would cause cracking in the interface region where some brittle aluminides such as Al_3Ni and AlNi are distributed, especially at the root edge between clad and substrate and at voids or inclusions in the interface region where stress concentration could occur, as shown in Fig. 14. An increase of T_s could reduce ΔT and thus reduce σ according to Eq 5. Simultaneously, preheating the substrate and increasing Al content from 0 to 3 wt% could reduce the contact angle (see Fig. 15, 16) and ease the stress concentration at the root edge. Therefore, the preheating of substrate and the addition of Al to the clad had a significant contribution to reducing ICR, as shown in Fig. 6 and 8. Unfortunately, an increase of Al content enlarged the brittleness of the clad due to the formation of some brittle aluminides, and the cracking trend increased with an increase of Al content, as shown in Fig. 7 and 9. An addition of only 1 wt% Al to the clad could produce crack-free clad without preheating of the substrate, because of both its lower brittleness and good matching property between the clad and the substrate.

From basic knowledge of thermodynamics of alloys, it is well known that the possible aluminides formed in the interface region were Al_xNi_y or Al_xFe_y, since Al has a stronger interaction with Ni and Fe than other elements existing in the interface region (Si, Cr, Cu, Mo) (Ref 8). Further comparison of Ni and Fe shows that the Gibbs free energy of Al-Fe aluminides is much larger than that of Al-Ni aluminides (Ref 8), as shown in Fig. 17. Therefore, the major aluminides formed in the interface region were Al-Ni aluminides rather than Al-Fe aluminides, although the content of Fe in the interface region is much higher than that of Ni, as indicated in Fig. 13. It can be found from Fig. 13 that the weight percent ratio of Al to Ni in most of the interface region was larger than 0.25. In this case, the possible aluminides are Al_3Ni, Al_3Ni_2, and AlNi, as indicated in the equilibrium binary Al-Ni phase diagram (Ref 8). But Al_3Ni_2 was unstable; it would decompose into Al_3Ni and AlNi (Ref 8):

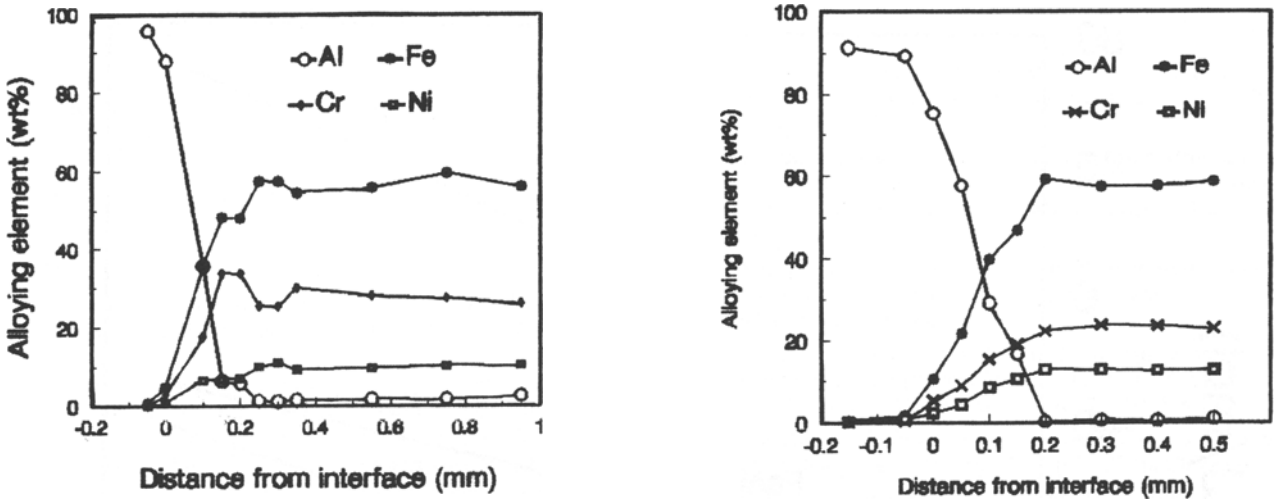

Fig. 13 Element distribution of laser-clad WF312 coating perpendicular to the substrate surface, cross-sectioned at: (a) T_S = 200 °C and (b) T_S = 300 °C

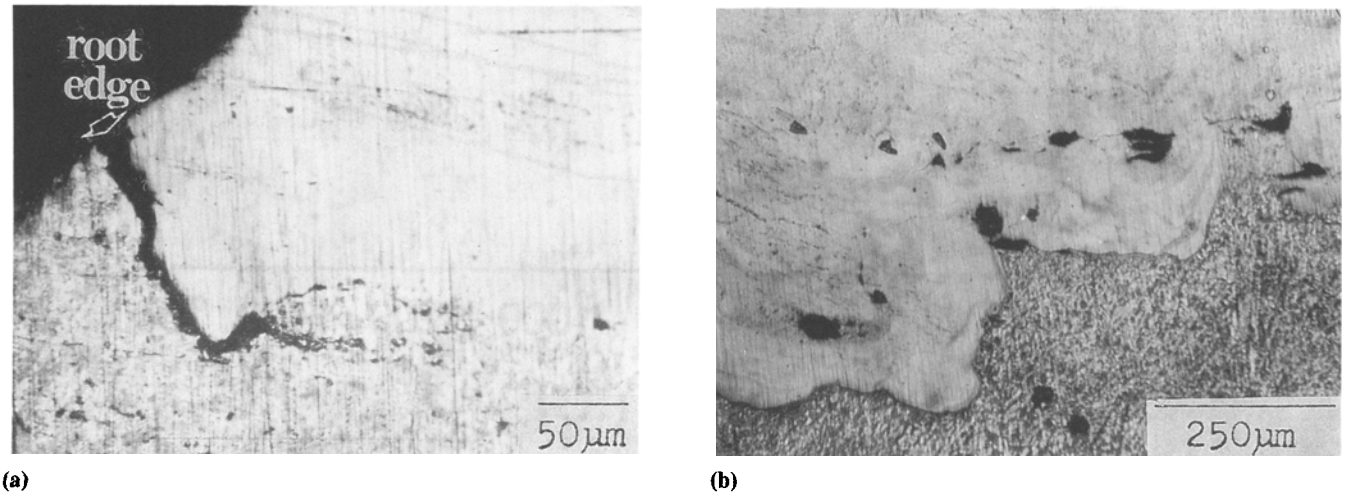

Fig. 14 Cracking at (a) the root edge between the clad and the substrate, and (b) at voids or inclusions

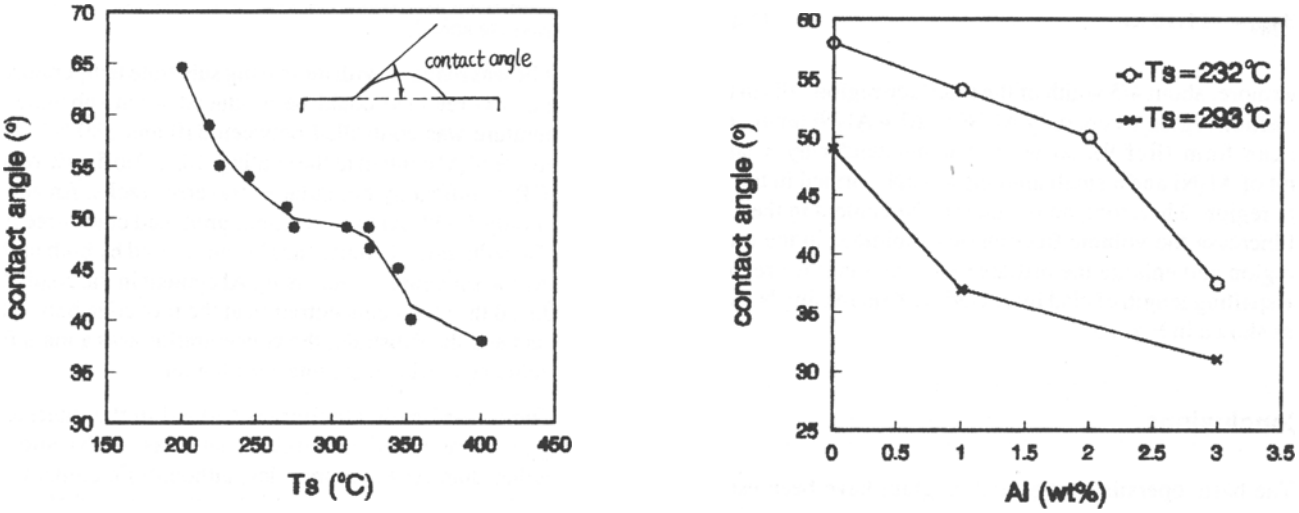

Fig. 15 Contact angle changing with T_S

Fig. 16 Contact angle changing with Al content at different T_S

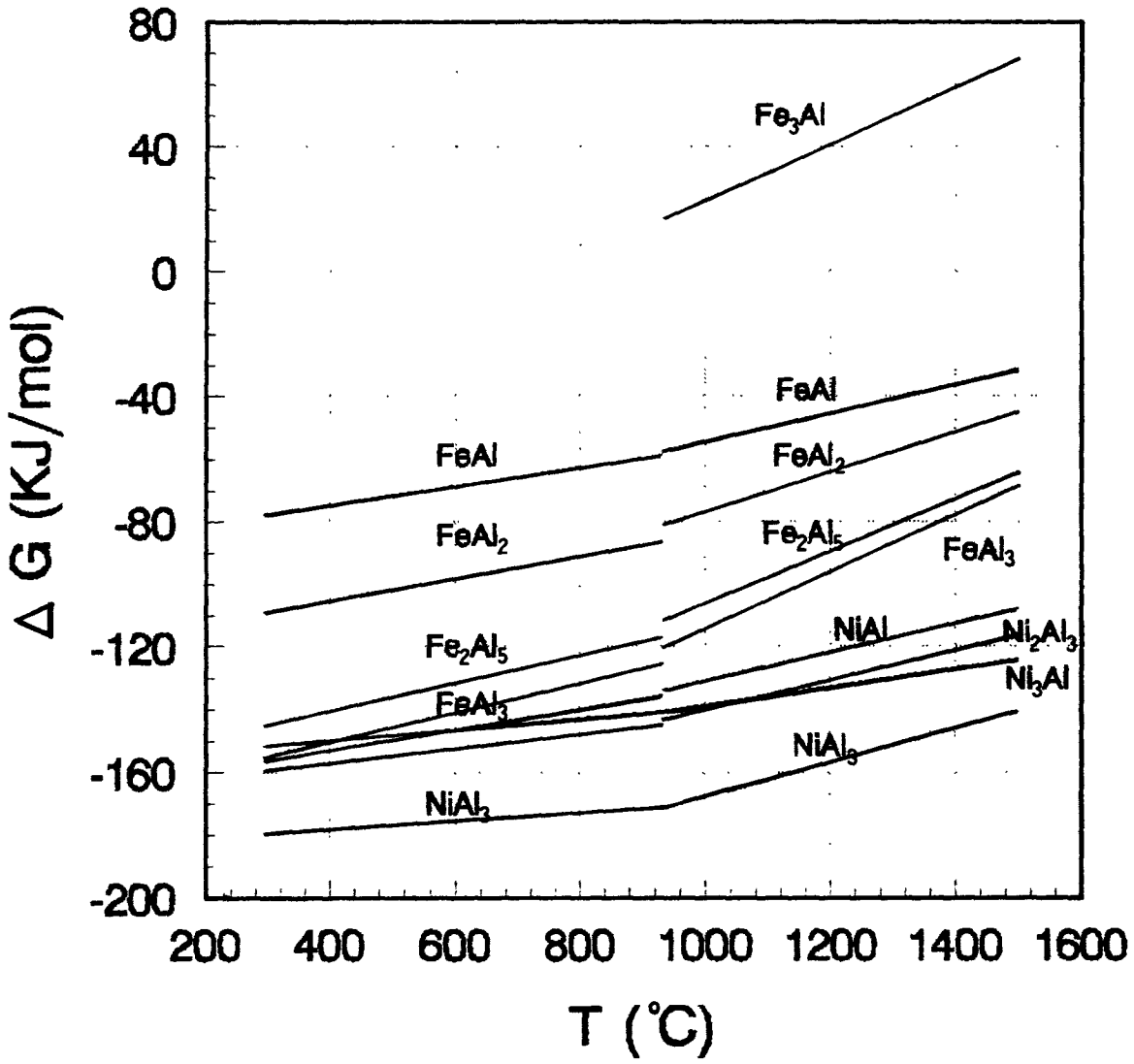

Fig. 17 Gibbs free energy of Al-Fe and Al-Ni aluminides changing with temperature

$$4/3\ Al_3Ni_2 \rightarrow 2/3\ Al_3Ni + 2NiAl$$
$$\Delta H_{289} = -11.18\ kJ \qquad \text{(Eq 6)}$$

Furthermore, about 4/5 width of the interface region falls in the composition region where only Al_3Ni or Al + Al_3Ni binary eutectic can form (Ref 9), so we can understand why a large amount of Al_3Ni and a small amount of AlNi formed in the interface region. Therefore, an increase of Ni content in the clad could increase the volume fraction of aluminides in the interface region and enlarge the brittleness of the interface region. So the spalling length of clad increased with increasing Ni content, as shown in Fig. 10.

5. Conclusions

- The basic operating range and diagram have been established for the laser cladding of iron-base alloy on Al-Si alloy substrate.
- Preheat temperature and tempering temperature had more significant influence on ICR than laser power and laser traverse speed.
- ICR was reduced with increasing substrate temperature and a crack-free clad could be produced when substrate temperature was controlled between 310 and 380 °C. An increase of Al content in the coatings from 0 to 5 wt% reduced ICR significantly but induced traverse cracks. An addition of only 1 wt% Al to the coating produced crack-free clads. The reduction of contact angle contributed by both preheating the substrate or increasing Al content in the coatings reduced the stress concentration at the root edge between the clad and the substrate; the concentration was a main factor inducing cracks in the interface region.
- The major brittle aluminides formed in the interface region were Al-Ni aluminides such as Al_3Ni and AlNi rather than Al-Fe aluminides, although Fe content in the interface region is much higher than that of Ni. An increase of Ni in the coatings increased the amount of brittle

aluminides and thus increased the amount of spalling of clad from the substrate.

Acknowledgments

This work was financially supported by the Natural Science Fund of China under the contract No. 59581004 and the Special Fund for Doctors Research of China.

References

1. J. Chen, A. Wang, and H. Dang, Friction Surface Modification of Aluminium Materials, *Tribology,* Vol 14, 1994, p 259-269 (in Chinese)
2. A. Houndri and S. Polymenis, Laser Melting Treatment by Overlapping Passes of Preheated Nickel Electrodeposited Coatings on Al-Si Alloy, *Metall. Trans. A,* Vol 23, 1992, p 1801-1806
3. M. Kawasaki, K. Takase, S. Kato, M. Nakagawa, K. Mori, M. Nemoto, S. Takagi, and H. Sugimoto, "Development of Engine Valve Seats Directly Deposited onto Aluminium Cylinder Head by Laser Cladding Process," Technical Paper 920571, presented at SAE Int. Congress and Exposition, Detroit, MI, 24-28 Feb 1992
4. Y. Liu, J. Mazumder, and K. Shibata, Laser Cladding of Ni-Al Bronze on Al Alloy AA333, *Metall. Mater. Trans. B,* Vol 25, 1994, p 749-759
5. Y. Liu, J. Mazumder, and K. Shibata, Microstructural Study of the Interface in Laser-Clad Ni-Al Bronze on Al Alloy AA333 and Its Relation to Cracking, *Metall. Mater. Trans. A,* Vol 26, 1995, p 1519-1533
6. Y.X. Li and W.M. Steen, Laser Cladding of Stellite and Silica on Aluminium Substrate, *Lasers and Optoelectronics,* Vol 1979, SPIE, 1992, p 602-608
7. Y. Liu, J. Koch, J. Mazumder, and K. Shibata, Processing, Microstructure, and Properties of Laser-Clad Ni Alloy FP-5 on Al Alloy AA333, *Metall. Mater. Trans. B,* Vol 25, 1994, p 430
8. B.P. Pabob, *Welding of Aluminium and Its Alloys with Other Metals,* Yuhang Press, Beijing, 1990, p 22-27 (in Chinese)
9. S. Tosto, P. Vanhile, and C. Vignaud, Ti Cladding and Ni Alloying on Pure Aluminum and Aluminum Alloys by an Electron Beam Technique, *Surf. Coat. Technol.,* Vol 58, 1993, p 141-142